Direct observation of band bending in the topological insulator Bi_2Se_3

C. E. ViolBarbosa,[1,*] Chandra Shekhar,[1] Binghai Yan,[1] S. Ouardi,[1] Eiji Ikenaga,[2] G. H. Fecher,[1] and C. Felser[1]

[1]*Max Planck Institute for Chemical Physics of Solids, Nöthnitzer Strasse 40, 01187 Dresden, Germany*

[2]*JASRI, SPring-8, Hyogo, 679-5198, Japan*

(Received 22 June 2013; revised manuscript received 26 August 2013; published 15 November 2013)

The surface band bending tunes considerably the surface band structures and transport properties in topological insulators. We present a direct measurement of the band bending on the Bi_2Se_3 by using the bulk sensitive angular-resolved hard x-ray photospectroscopy (HAXPES). We tracked the depth dependence of the energy shift of Bi and Se core states. We estimate that the band bending extends up to about 20 nm into the bulk with an amplitude of 0.23–0.26 eV, consistent with profiles previously deduced from the binding energies of surface states in this material.

DOI: 10.1103/PhysRevB.88.195128 PACS number(s): 79.60.Bm, 03.65.Vf

Topological insulators (TIs), a new quantum state, are characterized by robust metallic surface states inside the bulk energy gap, which are due to the topology of bulk band structures.[1–4] A large amount of effort was devoted to observe the topological surface states of many TI materials (Ref. 5 and references therein) by surface-sensitive experiments. Specially, Bi_2Se_3 is one of the most extensively studied TI materials because of its simple Dirac-type surface states and large bulk gap.[6–8]

Surface band bending (SBB) effects of Bi_2Se_3 have been commonly observed in angle-resolved photoemission spectra[8,9] (ARPES) and transport measurements.[10,11] The SBB is usually caused by surface degrading in ambient environment and surface doping,[12–15] with a downshift of the surface Dirac point, indicating an electron-doped surface.[16] SBB induces a quantum confinement effect[17] and modifies the surface and bulk bands dramatically. A clear feature of SBB in Bi_2Se_3 is a pair of Rashba-splitting bands above the Dirac cone.

In transport experiments, SBB is also supposed to affect the measurement in a considerable way by directly tuning the bulk and surface charge carrier densities.[11,18–20] So far, this surface band bending has only been deduced[13,14] from Rashba splitting of the conduction bands measured by ARPES, that is mainly sensitive to several surface atomic layers, although SBB is predicted to extend in an order of 10 nm distance from the surface into the bulk. A direct measurement of SBB from the surface into the bulk region is yet to be performed.

In this paper we reported the direct observation of SBB on the Bi_2Se_3 surface by hard x-ray photoelectron spectroscopy (HAXPES), a bulk sensitive method. The hard x-ray excitation ($\sim$8 keV) produces photoelectrons with high kinetic energy (E_{kin}) and consequently high inelastic mean free path (λ) resulting in an enhanced probing depth. HAXPES has been successfully utilized in the study of Heusler TIs.[21,22] The SBB can be directly measured in photoelectron spectroscopy by controlling the escape depth in the photoemission process to track the depth dependence of core level energies. Such controlling can be achieved by changing the photon energy and consequently the inelastic mean-free path, as demonstrated by Himpsel *et al.*[23] for low photon energy regime. The precision of this approach however depends on the energy distribution and the determination of the Fermi edges for different photon energies. Here we propose the angular-resolved HAXPES as an alternative to control the photoelectron escape depth, keeping constant all the experimental parameters: photon energy, incidence angle, and probed region. This is possible thanks to the high energy wide-acceptance objective lens setup specially developed for this purpose.[24,25] The objective lens enlarges the effective acceptance allowing the measurement of the photoelectron angular distribution with a fixed incident angle. In this work we measured the angular distribution of the photoemission of Bi_2Se_3 core levels, from where we observed the electric potential variations from bulk to surface.

Bi_2Se_3 single crystals were synthesized from a stoichiometry mixture of high purity (>99.99%) of bismuth (Bi) and selenium (Se). The elements were sealed in a dry quartz ampoule under a pressure of 10^{-6} Torr. The sealed ampoule was loaded into a vertical furnace and heated to 800 °C at a rate of 60 °C/h followed by 12 h of soaking. For a single crystal growth, the temperature was slowly reduced from 800 to 500 °C and thereafter by 100 °C/h to room temperature. This procedure resulted in silver-colored single crystals of 10 mm.

For HAXPES measurements, the crystal sample was exfoliated and kept in the air for a few seconds in order to ensure the saturation of the adsorption process at the surface, in such a way to eliminate any time-dependent effect. The experiment was performed at BL47XU at Spring-8 (Japan) using 7.94 keV photon energy and π linearly polarized light. The energy and angular distribution of the photoexcited electrons were analyzed using a high energy VG Scienta R4000-HV hemispherical analyzer. The objective lens, set in front of the analyzer, enlarges the effective acceptance angle to about 60° with an angular resolution of 1°. The homogeneity and precision of the system was checked by mapping the angular distribution of Au $4f$ peaks. The overall energy resolution was about 230 meV. The angle between the electron spectrometer and the photon propagation was fixed at 90°. Incoming photons were set to impinge on the sample at 60° from its surface normal, in such a way that the angular distribution of incoming electrons is measured from −2° to 62° with respect to the sample normal. Sample temperature was kept at 40 K. Figure 1(a) illustrates how the depth profile of core shift can be extracted from the angular distribution of the photoemission by considering an effective escape depth $\lambda^{\theta} = \lambda\cos(\theta)$, with θ being the emission angle. Figures 1(b) and 1(c) show the relationship between SBB and the depth dependence of a core level energy shift. The vertical bars in Fig. 1(c) indicate the energy position of the Se $2p_{3/2}$ peak

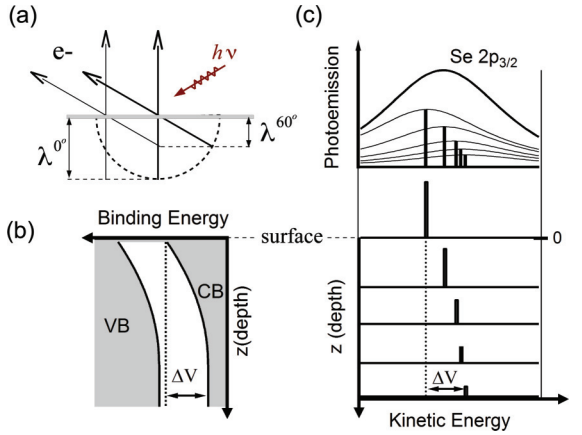

FIG. 1. (Color online) (a) Schematic of the experimental geometry. The angular distribution of photoemission is simultaneously measured in the range from 0 (normal) to 60°, being related with the electron escape depth λ^{θ}, where θ represents the emission angle. (b) Model for SBB in Bi_2Se_3, where ΔV represents the bending amplitude. (c) Representation of normal photoemission of Se $2p_{3/2}$. The vertical bars indicates the depth-dependent contribution of Se $2p_{3/2}$ to the normal photoemission.

for different depths. ΔV represents the bending amplitude in both figures. The depth dependence of the energy shift of core levels mimics the band bending profile.

Symbols in Fig. 2 represent the experimental energy distribution curves (EDCs) for Se $2p_{3/2}$ and Bi $3d_{5/2}$ core state photoemission. The spectra are summed up over slices of ±2° about the photoemission direction indicated by the label on the right of each curve. The curves were normalized by the peak intensity. Direct inspection of the EDCs indicates an energy shift in the core level peaks, as represented by the solid curved line. A total shift of −75(1) meV from $\theta = 0°$ to $\theta = 60°$ for both Se $2p_{3/2}$ and Bi $3d_{5/2}$ peaks was determined by Voigt function fitting. λ is calculated by the TPP-2M formula[26] to be $\lambda_{Bi} = \lambda(5.3\,\text{keV}) = 8.7$ nm and $\lambda_{Se} = \lambda(6.5\,\text{keV}) = 9.4$ nm for Bi $3d_{5/2}$ and Se $2p_{3/2}$, respectively. Providing the large electron escape depth and kinetic energies, the measured EDCs can only be originated by a bent potential which extends from the surface up to a distance of the same order of magnitude as λ. Therefore, the observed shifts indicate that bulk core levels ($z > z_l$) have smaller binding energy than core levels near to the surface ($z \sim 0$). This remarkable result consists in the direct observation of the band bending in Bi_2Se_3, indicating a downward bending from bulk to surface.

For a quantitative analysis, we model the angular distribution $I(\theta, E_{\text{kin}})$ by the following equation:

$$I(\theta, E_{\text{kin}}) = \int_0^{\infty} dz e^{-z/\lambda\cos(\theta)}\{\text{L}(\Gamma, b, E_0(z), E_{\text{kin}}) + I_0\}, \tag{1}$$

where I_0 represents the constant background, and L is a Lorenztian function:

$$L(\Gamma, b, E_0(z), E_{\text{kin}}) = \frac{\alpha}{\left(\frac{\Gamma}{2}\right)^2 + [E_{\text{kin}} - E_0(z)]^2} + b[E_{\text{kin}} - E_0(z)].$$

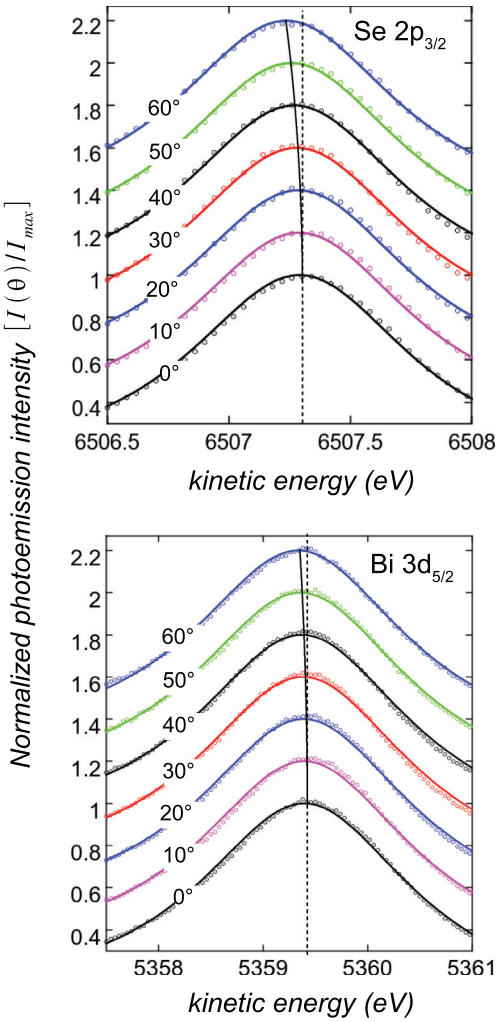

FIG. 2. (Color online) Energy distribution curves for Bi $3d_{5/2}$ (top) and Se $2p_{3/2}$. Symbols and solid lines represent experimental data and the calculated spectra $I(\theta, E_k)$, respectively. The energy shifts are indicated by the vertical solid and dashed lines.

The Lorentzian shape is given by b and Γ, representing the background asymmetry and spectral linewidth, respectively. The peak is centered in different energies E_0 according to the depth position z. $E_0(z)$ mimics the band bending (see Fig. 1). α is a normalization constant.

The band bending depth profile depends on detailed characteristics of the charge distribution near the surface. As a simplest approach we modeled the band bending profile as a quadratic function, extending for a distance $z = z_l$ from the surface ($z = 0$). This approach allows the evaluation of the extension z_l and strength ΔV of the band bending in Bi_2Se_3

TABLE I. Optimized parameters for Bi $3d_{5/2}$ and Se $2p_{3/2}$ peaks. The variation of $E_0(z)$ from bulk value is shown in Fig. 3.

Parameters	Bi $3d_{5/2}$	Se $2p_{3/2}$
E_0^{bulk}	5359.52(2) eV	6507.40(2) eV
Γ	2.47(1) eV	1.20(1) eV
b	$-0.40(8) \times 10^{-2}$	$-3.20(10) \times 10^{-2}$

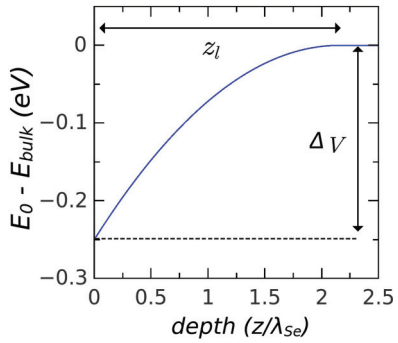

FIG. 3. (Color online) Energy shift depth profile for Se $2p_{3/2}$ and Bi $3d_{5/2}$. The energy shift profile mimics the band bending in the Bi_2Se_3.

by refining $E_0(z)$:

$$E_0(z) = \begin{cases} \frac{\Delta V}{z_l}[z - z_l]^2 + E_0^{\text{bulk}}, & z < z_l, \\ E_0^{\text{bulk}}, & z \geqslant z_l. \end{cases} \quad (2)$$

For comparison with the experimental data, the calculated spectra $I(\theta, E_{\text{kin}})$ were convoluted with a Gaussian representing the total energy resolution (FWHM = 230 meV). The curves were refined by the minimization of the mean square error (MSE). The optimized parameters for Se $2p_{3/2}$ and Bi $3d_{5/2}$ peaks are summarized in Table I. The optimum values for z_l and ΔV are, respectively, $2.13\lambda_{\text{Se}}$ (or $2.29\lambda_{\text{Bi}}$) and 0.25 eV. The calculated spectra $I(\theta, E_k)$ using optimum parameters are shown in Fig. 2 as solid lines. Figure 3 shows the depth dependence of the energy shift of both core levels, as derived from $\Delta V(z) = [E_0(z) - E_0^{\text{bulk}}]$. The z axis is shown normalized by the λ_{Se}. The uncertainty in the estimation of $E_0(z)$ was calculated by finding the confidence intervals of its parameters (ΔV,E_0^{bulk},z_l), in which the MSE variation is smaller than 1%. It resulted in the regions $z_l\lambda_{\text{Se}} = 1.8$–$2.4$ and $\Delta V = 0.23$–0.26 eV. Therefore, our model suggests that the band banding extends to $z_l \approx 2\lambda$ (about 20 nm). These results are in agreement with the band bending inferred from surface states position in ARPES measurements.[13,14]

In summary, we have observed the band bending Bi_2Se_3 by measuring the angular dependence of high energy photoelectrons emitted from core levels. The angular dispersions in kinetic energy were modeled as originated from a depth-dependent shift in binding energy of core states. The depth profile of core shifts was extracted in a single experiment from the angular distribution of photoelectrons. We found a downward band bending of about 0.25 eV, which extends to approximately 20 nm into the crystal, in good agreement with the values deduced from ARPES measurements.[13,14] Finally, it should be emphasized that the use of the angle-resolved HAXPES in wide angle allows the deeply probing of bulk states and opens the avenue for investigation of band bending and interface potential in multilayered structures.

This work was financially supported by the Deutsche Forschungsgemeinschaft (DFG, German Research Foundation) within the priority program SPP1666 "Topological insulators." The synchrotron radiation measurements were performed at BL-47XU with the approval of the Japan Synchrotron Radiation Research Institute (JASRI) (Proposal No. 2012A0043).

*carlos.barbosa@cpfs.mpg.de

[1] X. Qi and S. Zhang, Phys. Today **63**, 33 (2010).
[2] J. Moore, Nature (London) **464**, 194 (2010).
[3] M. Z. Hasan and C. L. Kane, Rev. Mod. Phys. **82**, 3045 (2010).
[4] X.-L. Qi and S.-C. Zhang, Rev. Mod. Phys. **83**, 1057 (2011).
[5] B. Yan and S.-C. Zhang, Rep. Prog. Phys. **75**, 096501 (2012).
[6] H. Zhang, C.-X. Liu, X.-L. Qi, X. Dai, Z. Fang, and S.-C. Zhang, Nat. Phys. **5**, 438 (2009).
[7] Y. Xia, D. Qian, D. Hsieh, L. Wray, A. Pal, H. Lin, A. Bansil, D. Grauer, Y. S. Hor, R. J. Cava, and M. Z. Hasan, Nat. Phys. **5**, 398 (2009).
[8] Y. Chen, J. Chu, J. Analytis, Z. Liu, K. Igarashi, H. Kuo, X. Qi, S. Mo, R. Moore, D. Lu *et al.*, Science **329**, 659 (2010).
[9] D. Hsieh, Y. Xia, D. Qian, L. Wray, J. Dil, F. Meier, J. Osterwalder, L. Patthey, J. Checkelsky, N. Ong *et al.*, Nature (London) **460**, 1101 (2009).
[10] D. Kong, J. J. Cha, K. Lai, H. Peng, J. G. Analytis, S. Meister, Y. Chen, H.-J. Zhang, I. R. Fisher, Z.-X. Shen, and Y. Cui, ACS Nano **5**, 4698 (2011).
[11] J. G. Checkelsky, Y. S. Hor, R. J. Cava, and N. P. Ong, Phys. Rev. Lett. **106**, 196801 (2011).
[12] M. Bianchi, D. Guan, S. Bao, J. Mi, B. Iversen, P. King, and P. Hofmann, Nat. Commun. **1**, 128 (2010).
[13] P. D. C. King, R. C. Hatch, M. Bianchi, R. Ovsyannikov, C. Lupulescu, G. Landolt, B. Slomski, J. H. Dil, D. Guan, J. L. Mi, E. D. L. Rienks, J. Fink *et al.*, Phys. Rev. Lett. **107**, 096802 (2011).
[14] H. M. Benia, C. Lin, K. Kern, and C. R. Ast, Phys. Rev. Lett. **107**, 177602 (2011).
[15] D. Hsieh, J. W. McIver, D. H. Torchinsky, D. R. Gardner, Y. S. Lee, and N. Gedik, Phys. Rev. Lett. **106**, 057401 (2011).
[16] M. Koleini, T. Frauenheim, and B. Yan, Phys. Rev. Lett. **110**, 016403 (2013).
[17] M. S. Bahramy, P. D. C. King, A. de la Torre, J. Chang, M. Shi, L. Patthey, G. Balakrishnan, P. Hofmann, R. Arita, N. Nagaosa, and F. Baumberger, Nat. Commun. **3**, 1159 (2012).
[18] H. Steinberg, D. R. Gardner, Y. S. Lee, and P. Jarillo-Herrero, Nano Lett. **10**, 5032 (2010).
[19] F. Xiu, L. He, Y. Wang, L. Cheng, L.-T. Chang, M. Lang, G. Huang, X. Kou, Y. Zhou, X. Jiang, Z. Chen, J. Zou *et al.*, Nat. Nanotechnol. **6**, 216 (2011).

[20]D. Kim, S. Cho, N. P. Butch, P. Syers, K. Kirshenbaum, S. Adam, J. Paglione, and M. S. Fuhrer, Nat. Phys. **8**, 460 (2012).
[21]S. Ouardi, C. Shekhar, G. H. Fecher, X. Kozina, G. Stryganyuk, C. Felser, S. Ueda, and K. Kobayashi, Appl. Phys. Lett. **98**, 211901 (2011).
[22]C. Shekhar, S. Ouardi, G. H. Fecher, A. Kumar Nayak, C. Felser, and E. Ikenaga, Appl. Phys. Lett. **100**, 252109 (2012).
[23]F. J. Himpsel, G. Hollinger, and R. A. Pollak, Phys. Rev. B **28**, 7014 (1983).
[24]H. Matsuda and H. Daimon, Patent PCT/jp2004/016602 Japan 208926 (2004).
[25]H. Matsuda, H. Daimon, M. Kato, and M. Kudo, Phys. Rev. E **71**, 066503 (2005).
[26]S. Tanuma, C. J. Powell, and D. R. Penn, Surf. Interface Anal. **21**, 165 (1994).